Max-Planck-Gesellschaft
zur Förderung der Wissenschaften e.V.

Arbeitsgruppe Mechanik heterogener Festkörper
an der Technischen Universität Dresden

Report MPG/DD1/931110

A Dynamically Adaptive Grid Method for Solving One-Dimensional Non-Stationary Partial Differential Equations

by

V. I. Mazhukin
M. Bobeth
U. Semmler

Dresden, 10. 11. 1993

A Dynamically Adaptive Grid Method for Solving One–Dimensional Non–Stationary Partial Differential Equations

V. I. Mazhukin[1], M. Bobeth[2], and U. Semmler[3]

[1]The Institute for Mathematical Modelling, Russian Academy of Sciences, Moscow, Russia

[2]Max–Planck–Gesellschaft, Arbeitsgruppe "Mechanik heterogener Festkörper", Dresden, Germany

[3]Gesellschaft für Fertigungstechnik und Entwicklung Schmalkalden, Institut für Werkzeugtechnik und Qualitätssicherung, Germany

Abstract

A dynamically adaptive grid method for solving partial differential equations exhibiting strong spatio–temporary solution variations is proposed. The method is based on a time–dependent coordinate transformation from the physical to a computational space which is controlled by the evolving solution. The transformation is determined by the condition that the solution in the computational space behaves nearly stationary. For the example of the Burgers' equation, describing convective and diffusive transport processes, an analytical investigation of the accuracy as well as the dispersive and dissipative properties of the method for different finite–difference schemes reveals that dispersion is strongly suppressed. As a consequence, a high computational efficiency compared to conventional calculations on a fixed grid is achieved.

1 Introduction

The problem of an appropriate grid generation for solving partial differential equations (PDEs) is of great current interest [1] – [6]. The accuracy of numerical solutions depends on how the distribution of grid points is adapted to the behaviour of the solution. For fixed number of grid points, a higher accuracy results by means of a distribution that is better matched to the peculiarities of the solution. In order to achieve an optimal distribution of grid points, numerous approaches to the generation of adaptive grids have been proposed [7] – [16].

For stationary problems, the peculiarities of the solution like strong gradients, discontinuities at boundaries etc. are spatially localized in general. This simplifies essentially the generation of adaptive grids. The accuracy of the numerical solution is improved by a higher density of grid points in regions of large solution variations [7] – [12].

For non–stationary problems like evolution equations, the generation of adaptive grids is more complicated since the peculiarities of the solution may appear, move and disappear in the course of time in the whole region where the solution is defined. In these cases, the appropriate distribution of grid points is not only related to the problem of increasing the accuracy but sometimes also to the problem of finding the proper qualitative behaviour of the solution. One of the most essential features for the generation of dynamically adaptive grids is the optimal choice of the grid point velocities. If the velocity is too slow, the grid points cannot follow the temporal changes of the solution which decreases the accuracy and efficiency of the procedure. On the other hand, an inappropriate fast movement of grid points can affect erroneous oscillations of the solution, or coupled oscillations of grid and solution, or the numerical calculation becomes globally unstable.

The efficiency of time–dependent adaptive algorithms depends crucially on the appropriate control of the grid movement by the evolving solution. Without any correlation, a new grid is generated after a certain number of time steps. This is sufficient if the solution evolves into a quasi–stationary asymptotic stage. For strong temporary changes of the solution, a grid rearrangement at every time step may be advantageous. This is typical for dynamically adaptive methods where the solution and the movement of the grid points are calculated simultaneously [17] – [20].

In the present work, a new procedure for the generation of a dynamically adaptive grid is proposed which is especially suited for the solution of one–dimensional non–stationary PDEs. As an illustration, the method is applied to the numerical solution of the Burgers' equation which describes transport processes by convection and diffusion. The difficulties in the solution of similar equations by means of conventional methods are well–known [21, 22]. Application of difference schemes of first order accuracy, $O(\tau + h^2)$, in connection with an insufficient grid point density leads to an increase of the numerical viscosity in the region of strong gradients and, therefore, to a strong smoothing of the solution. Difference schemes of second order, $O(\tau^2 + h^2)$, affect strong oscillations of the solution. In some cases, one cannot avoid the appearance of oscillations.

2 Idea of the Method

The present adaptive method is based on a time–dependent coordinate transformation (TDCT) from the physical space to a computational space. The numerical solution of a PDE is formulated by two coupled differential equations, where one equation describes the physical process and the other one the movement of the grid points in the physical space. The essential point is that the TDCT is governed in an appropriate manner by the evolving solution.

Previously, TDCTs have been applied mostly in order to desribe properly moving boundaries as well as special lines and surfaces in aero- and hydrodynamics [1]. In those cases, the grid has been adapted to peculiarities of the solution like shock waves [23, 24], internal phase boundaries [25, 26], and free surfaces [27, 28], but not to the gradient of the solution. A well–known example for the application of a TDCT are the classical Lagrange coordinates in hydrodynamics where the velocity of the coordinate movement is determined by the hydrodynamic flow velocity. Recently, a modified method of Lagrange coordinates has been applied also to an adaptation to the gradient of the solution [16]. In [16], the control of the grid movement has been connected with the requirement of equidistributing the second derivative of the solution.

The TDCT presented here allows us to generate a moving grid which is able to adapt to various peculiarities of the solution including large gradients [18, 29], moving boundaries [17, 30] as well as shock waves [19].

In the following, the special procedure for generating the moving grid is explained. Let us consider a TDCT from the physical space (x,t) to the computational space (q,T) given by the relations $x = f(q,T)$ and $t = T$. The transformation is to possess the non–degenerate back transformation $q = \phi(x,t)$ and $T = t$. The partial derivatives with respect to the independent variables are given by

$$\frac{\partial}{\partial t} = \frac{\partial}{\partial T} + \frac{\partial q}{\partial t}\frac{\partial}{\partial q} = \frac{\partial}{\partial T} - \frac{\partial x}{\partial T}\frac{1}{\Psi}\frac{\partial}{\partial q} \equiv \frac{\partial}{\partial T} + \frac{Q}{\Psi}\frac{\partial}{\partial q}, \tag{1}$$

$$\frac{\partial}{\partial x} = \frac{\partial q}{\partial x}\frac{\partial}{\partial q} \equiv \frac{1}{\Psi}\frac{\partial}{\partial q}, \qquad \frac{\partial^2}{\partial x^2} = \frac{1}{\Psi}\frac{\partial}{\partial q}\frac{1}{\Psi}\frac{\partial}{\partial q} \tag{2}$$

where $\Psi = \partial x/\partial q$ is the metric coefficient and $\partial x/\partial T$ describes the movement of the physical coordinate for fixed coordinate q. The computations are performed on a fixed grid in the (q,T) space. The corresponding movement of grid points in the physical space (x,t) is formally determined by the function $Q(q,T)$ which defines the coordinate back transformation

$$\frac{\partial x}{\partial T} = -Q. \tag{3}$$

In some cases, it is more convenient to use the following relation

$$\frac{\partial \Psi}{\partial T} = -\frac{\partial Q}{\partial q} \tag{4}$$

which is obtained from (3) by applying $\partial/\partial q$. The crucial step now is to relate the function Q suitably to the evolving solution in order to achieve an optimal adaptation.

The success of the method of dynamically adaptive grids depends on the proper choice of the properties of the solution which serve for the control of the grid movement. Usually, the approximation error of the solution or its derivatives are used. In the following, an alternative approach is proposed. From the analysis of finite–difference schemes it is well–known that the dissipative and dispersive properties of difference schemes are essentially determined by the time derivative. This circumstance suggests that a TDCT into a coordinate system where the time derivative of the solution is equal to zero or sufficiently small is advantageous. For this reason we choose in the following the TDCT defined by

$$\frac{\partial u}{\partial T} = 0. \tag{5}$$

The requirement (5) also defines the function $Q(q,T)$ via the PDE and, consequently, Q is determined by the evolving solution. The special form of Q depends of course on the PDE under consideration.

In order to illustrate the present approach, let us consider the Burgers' equation

$$\frac{\partial u}{\partial t} + \frac{\partial}{\partial x}\frac{u^2}{2} = \mu \frac{\partial^2 u}{\partial x^2}, \tag{6}$$

a one–dimensional nonlinear PDE of Navier–Stokes type, with $x_a < x < x_b$, $t \geq 0$, and the following initial and boundary conditions

$$u(x,0) = u^0(x), \qquad t = 0, \tag{7}$$

$$g_a(x,t,u,\partial u/\partial x) = 0, \qquad x = x_a, \quad t > 0, \tag{8}$$

$$g_b(x,t,u,\partial u/\partial x) = 0, \qquad x = x_b, \quad t > 0. \tag{9}$$

The Burgers' equation is often used to test the accuracy and computational efficiency of numerical solution procedures because the solution of this equation evolves like a shock wave for small viscosity parameter μ ($\mu < 10^{-3}$).

By using relations (1) – (4), the Burgers' equation in the (q,T) coordinates is expressed as

$$\frac{\partial u}{\partial T} + \frac{Q}{\Psi}\frac{\partial u}{\partial q} + \frac{1}{\Psi}\frac{\partial}{\partial q}\frac{u^2}{2} = \frac{1}{\Psi}\frac{\partial}{\partial q}\frac{\mu}{\Psi}\frac{\partial u}{\partial q} \tag{10}$$

and the relation to the physical coordinate x is given by

$$\frac{\partial x}{\partial q} = \Psi, \qquad \frac{\partial \Psi}{\partial T} = -\frac{\partial Q}{\partial q}, \qquad q_a < q < q_b, \quad T > 0. \tag{11}$$

According to the definition of the TDCT by the requirement (5) together with the PDE (10), the function Q is obtained as

$$Q = \left(\frac{\partial u}{\partial q}\right)^{-1}\left[\frac{\partial}{\partial q}\frac{\mu}{\Psi}\frac{\partial u}{\partial q} - \frac{\partial}{\partial q}\frac{u^2}{2}\right] = -u + \frac{\partial}{\partial q}\frac{\mu}{\Psi} + \frac{\mu}{\Psi}\left(\frac{\partial u}{\partial q}\right)^{-1}\frac{\partial^2 u}{\partial q^2}. \tag{12}$$

In the following, the efficiency of the numerical solution of (10) by using an appropriate function Q is investigated both analytically and numerically. To this end, the discrete space ω_h^τ is introduced

$$\omega_h^\tau = \{(q_i, q_{i+1/2}, T^j) : \; q_{i+1} = q_i + h, \; q_{i+1/2} = q_i + h/2, \;\; i = 0, 1, \ldots I-1,$$

$$T^{j+1} = T^j + \tau^j, \;\; j = 0, 1, 2 \ldots \} \tag{13}$$

and equations (10) and (11) are approximated by finite–difference schemes. However, in order to demonstrate the insensibility of the procedure to a slight violation of condition (5), the numerical calculations presented here have been performed with a slightly modified function Q neglecting the third term on the r. h. s. in (12).

3 Analysis of Difference Approximations to the Transformed PDE

Consider different three–point two–shell difference approximations to the Burgers' equation (10) in the (q, T) coordinate system

$$u_T = -\left[\frac{Q}{\Psi} u_{q,\alpha} + \frac{1}{2\Psi}(u^2)_{q,\alpha} - \frac{\mu}{\Psi}\left(\frac{1}{\Psi} u_{q,f}\right)_{q,b}\right]_\sigma \tag{14}$$

where

$$u_T = (u_i^{j+1} - u_i^j)/\tau^j. \tag{15}$$

The index α = c, f, b denotes the central, forward and backward differences

$$\begin{aligned} f u_{q,c} &= f_i \, (u_{i+1} - u_{i-1})/2h, \\ f u_{q,f} &= f_i \, (u_{i+1} - u_i)/h, \\ f u_{q,b} &= f_i \, (u_i - u_{i-1})/h, \end{aligned} \tag{16}$$

and according to

$$[f]_\sigma = (1-\sigma) f^j + \sigma f^{j+1}, \qquad 0 \le \sigma \le 1 \tag{17}$$

the index σ controls whether the difference scheme is explicit ($\sigma = 0$), implicit ($\sigma = 1$) or of mixed type. The accuracy of the corresponding schemes is of order $O(\tau^k + h^l)$ with $k = 2$ for $\sigma = 1/2$ (symmetric Crank–Nicholson scheme), $k = 1$ for $\sigma = 0$ or 1, $l = 2$ for central differences in the space coordinate, and $l = 1$ else.

Because of requirement (5), defining the function Q, the transformed PDE (10) becomes stationary and the corresponding difference schemes read

$$Q \, u_{q,\alpha} + \frac{1}{2}(u^2)_{q,\alpha} - \left(\frac{\mu}{\Psi} u_{q,f}\right)_{q,b} = 0, \qquad \alpha = c, \; f, \; b. \tag{18}$$

In the following, the accuracy of the difference approximations (18) is investigated analytically. The difference between the PDE and its finite–difference approximation can be considerable in certain cases. Since the approximation by finite differences corresponds to the replacement of an infinite–dimensional space of functions with continuous arguments by a finite–dimensional space of discrete grid functions, the solutions of the PDE and of the difference scheme belong to different functional spaces and, therefore, a comparison is complicated. Usually, it is assumed that the difference scheme is solved by functions of continuous arguments not only in the grid points, but in all points of the considered region of the solution. This allows us to transform difference operators into a functional space which includes also differential operators. In this way, difference schemes can be analyzed by methods developed for differential equations. As a result of the transformation of the difference scheme to a differential equation, the so–called "modified equation" is obtained [31, 32].

The modified equations corresponding to the difference schemes (18) are derived in a standard way by the expansion of the grid function in the vicinity of the grid point (q_i, T^j) into a Taylor series. Since the calculations are straightforward but involved, only the final results for the modified equations are given here

$$Q\frac{\partial u}{\partial q}+\frac{\partial}{\partial q}\frac{u^2}{2}-\frac{\partial}{\partial q}\frac{\mu}{\Psi}\frac{\partial u}{\partial q}= \tag{19}$$

$$=\alpha_\alpha\frac{\partial^2 u}{\partial q^2}+\beta\frac{\partial^3 u}{\partial q^3}+\gamma\frac{\partial^4 u}{\partial q^4}+\delta\frac{\partial^3}{\partial q^3}\frac{1}{\Psi}+\epsilon_\alpha\left(\frac{\partial u}{\partial q}\right)^2+R,\qquad R=O(h^m)$$

with

$$\alpha_c=-\frac{h^2}{8}\left[4\frac{\partial u}{\partial q}-\frac{\partial^2}{\partial q^2}\frac{\mu}{\Psi}\right],\quad \alpha_f=\alpha_c-(Q+u)\,h/2,\quad \alpha_b=\alpha_c+(Q+u)\,h/2,$$

$$\beta=\frac{h^2}{6}\left[\frac{\partial}{\partial q}\frac{\mu}{\Psi}-u-Q\right],\quad \gamma=\frac{h^2}{12}\frac{\mu}{\Psi},\quad \delta=\mu\frac{h^2}{24}\frac{\partial u}{\partial q},$$

$$\epsilon_c=0,\quad \epsilon_f=-h/2,\quad \epsilon_b=h/2.$$

($m=4$ for central differences, $m=3$ else). Note that it is important to investigate just the modified equations (19) since these equations are solved actually by the finite–difference scheme but not the starting PDE (10).

The numerical dissipation and dispersion of the difference schemes (18) are mainly given by the terms with the second and third derivative on the r. h. s. of (19), respectively [22, 31]. The corresponding coefficients α and β in these terms depend on the function Q. For example, the dispersion is of the order of R if one requires $\beta=O(h^m)$ which leads to

$$Q=-u+\frac{\partial}{\partial q}\frac{\mu}{\Psi}+O(h^{m-2}). \tag{20}$$

The choice (12) of the function Q fulfills this requirement. The simpler form

$$Q=-u+\frac{\partial}{\partial q}\frac{\mu}{\Psi} \tag{21}$$

would even lead to $\beta = 0$. It must be mentioned, however, that (21) implies a weak instationarity of the transformed equation ($\partial u/\partial T \neq 0$) so that (19) does not apply to this case rigorously. The modified equation corresponding to (21) is more complicated in comparison with (19) and requires extensive calculations. Note, however, that the calculations in the following section are carried out with the simpler transformation (21). The results show that the proposed procedure can be applied succesfully also if the choice of the function Q does not rigorously fulfill the stationarity condition (5).

The lowest dissipation of the difference schemes (18) is obtained for central differences ($\alpha_c = \mathrm{O}(h^2)$ compared to α_b, $\alpha_f = \mathrm{O}(h)$). Thus, the central difference scheme is in principle the most accurate approximation due to small numerical dissipation and very small dispersion. For difference schemes of the Burgers' equation on a conventional fixed grid, a small dissipation is disadvantageous since it cannot suppress numerical oscillations due to the relatively strong dispersion in this case. For the forward and backward difference schemes, the dissipation coefficient α contains a term $\sim (Q+u)\,h$ and, by inserting (12), this term becomes proportional to the physical viscosity μ. As a consequence, in the limiting case of small physical viscosity, the three difference schemes (18) show a similar behaviour. For high physical viscocity, the numerical dissipation plays no role since steep gradients in the solution are suppressed by the physical dissipation.

Finally, let us summarize the main conclusions of the present analysis:
(i) By an appropriate choice of the function Q, a TDCT can be determined so that the solution in the computational space behaves nearly stationary. (ii) Explicit and implicit schemes are equally suited for the present adaptation procedure. (iii) Dynamical adaptation can considerably increase the quality of the difference schemes. By means of the proposed procedure, it is possible to suppress strongly the dispersion and, simultaneously, to decrease considerably the degree of dissipation for first–order difference schemes in h.

4 Numerical Examples

The computational efficiency of the proposed adaptation procedure is illustrated in the following by the numerical solution of the Burgers' equation (6). The results are compared with the theoretical predictions of the above analysis of the modified equation as well as with results of conventional calculations on a fixed grid.

In the computational space (q, T), the Burgers' equation (10) is written in the divergent form

$$\frac{\partial(\Psi u)}{\partial T} = -\frac{\partial P(u)}{\partial q} - \frac{\partial(Qu)}{\partial q} \tag{22}$$

where

$$P(u) = -\frac{u^2}{2} - \frac{\mu}{\Psi}\frac{\partial u}{\partial q}. \tag{23}$$

The back transformation to the physical space (x, t) is given by (11). The function Q may be chosen according to (12) or (21).

The difference scheme is formulated on the grid (13) in the (q,T) coordinate system. The grid functions x_i^j, u_i^j and Q_i^j are calculated at the points (q_i,T^j) and, analogously, $\Psi_{i+1/2}^j$ and $P_{i+1/2}^j$ at $(q_{i+1/2},T^j)$. With the function Q according to (21), equations (22), (11) and (23) are approximated by the following difference equations

$$(\Psi u)_i^{j+1} = (\Psi u)_i^j - \frac{\tau^j}{h}\{(1-\sigma)[P_{i+1/2} - P_{i-1/2} + (uQ)_{i+1/2} - (uQ)_{i-1/2}]^j$$

$$+ \sigma\,[P_{i+1/2} - P_{i-1/2} + (uQ)_{i+1/2} - (uQ)_{i-1/2}]^{j+1}\}, \tag{24}$$

$$\Psi_{i+1/2}^{j+1} = \Psi_{i+1/2}^j - \frac{\tau^j}{h}\{(1-\sigma)[Q_{i+1} - Q_i]^j + \sigma\,[Q_{i+1} - Q_i]^{j+1}\}, \tag{25}$$

$$\frac{x_{i+1} - x_i}{h} = \Psi_{i+1/2}, \tag{26}$$

$$P_{i+1/2} = \frac{u_{i+1/2}^2}{2} - \frac{\mu}{\Psi_{i+1/2}}\frac{u_{i+1} - u_i}{h}, \qquad Q_i = -u_i + \frac{\mu}{h}\left(\frac{1}{\Psi_{i+1/2}} - \frac{1}{\Psi_{i-1/2}}\right). \tag{27}$$

The approximation error of this scheme is of the order $O(\tau + h^2)$ for $\sigma = 0,\ 1$ and of the order $O(\tau^2 + h^2)$ for $\sigma = 1/2$. The system of difference equations (24) - (27) has been solved by the Newton–Raphson iteration method. At every iteration step the system of linear algebraic equations with tridiagonal matrices can be solved easily. The time increment τ^j is controlled automatically by the required accuracy and by the number of iterations per time step.

Let us consider two typical examples which are often met in solving the Burgers' equation [14]. In both cases a small physical viscosity is assumed ($\mu = 10^{-4}$) so that the solution tends to form a discontinuity. Because of the special choice of the initial conditions $u^0(x)$, a quasi-discontinuity appears in the first example within the considered region of the solution, and in the second example at the boundary.

Example 1: The initial condition is chosen as an asymmetric sinusoidal function

$$u(x,0) = u^0(x) = \sin(2\pi x) + 0.5\,\sin(\pi x), \qquad 0 \le x \le 1 \tag{28}$$

and the boundary conditions are given by

$$u(0,t) = u(1,t) = 0, \qquad t > 0. \tag{29}$$

In the (q,T) coordinate system the following initial and boundary conditions for the solution of equations (11) have to be added

$$\Psi(q,0) = 1, \qquad 0 \le q \le 1, \tag{30}$$

$$Q(0,T) = Q(1,T) = 0, \qquad T > 0. \tag{31}$$

At first, the Burgers' equation (6) subject to conditions (28) and (29) has been solved numerically on a fixed grid in the (x,t) coordinate system. The calculations showed that on grids with less than 100 points the numerical solution is practically unstable.

The solution obtained with 1000 grid points is shown in Fig. 1. The two half–waves of the sine–function move to each other and form rapidly a steep front at which erroneous oscillations appear. Similar oscillations have been found also on the other side of the front if the number of grid points is less than 500. An increase of the number of grid points up to 10^4 diminishes the amplitude of the oscillations but they do not disappear (cf. Fig. 2). These results reveal a strong dispersion of the difference scheme applied.

By the use of the present adaptive grid method, solutions without oscillations have been obtained even with a relatively small number of grid points $I > 15$. For a point number of $I = 25$, the solution of the difference scheme (24) – (27), corresponding to the PDEs (22) and (11), is shown in Fig. 3 at the same times as in Figs. 1 and 2. The absence of oscillations is achieved by the appropriate movement of grid points controlled by the evolving solution. As discussed above, this can lead to the nearly complete disappearance of the numerical dispersion. As a consequence, calculations with a dynamically adaptive grid need unusually small numbers of grid points only.

In agreement with the theoretical predictions above, schemes of order $O(\tau + h^2)$ yield the same results as the scheme of order $O(\tau^2 + h^2)$. The only difference is that the second–order scheme in τ permits an about two times larger time increment.

The movement of grid points may conveniently be characterized by the function Ψ, which shows how the intervals Δx_i in the physical space expand ($\Psi > 1$) or shrink ($\Psi < 1$) in the course of time (cf. Fig. 4). The positions x_i are labeled by markers in Figs. 3 and 4. The grid points are concentrated in regions of large gradients of the solution. According to the plot in Fig. 4, some intervals shrink up to a factor of 1000 whereas other intervals expand up to a factor of 4.

Example 2: The initial condition is chosen similar to a step function

$$u^0(x) = \begin{array}{ll} 1, & 0 \le x \le 0.28 \\ 15 - 50x, & 0.28 < x < 0.3 \\ 0, & 0.3 \le x \end{array} \tag{32}$$

and the boundary conditions are given by

$$u(0,t) = 1,\ u(\infty,t) = 0, \qquad t > 0. \tag{33}$$

The initial and boundary conditions for equation (11) read

$$\Psi(q,0) = 1, \qquad 0 \le q, \tag{34}$$

$$Q(0,T) = Q(\infty,T) = 0, \qquad T > 0. \tag{35}$$

Unlike the first example, the solution exhibits a quasi–discontinuity already at the beginning, which moves along the x–axis in the course of time.

The method of dynamically adaptive grids has been applied to a series of problems with weak moving quasi–discontinuities as e. g. temperature waves [20, 29] as well as to strong discontinuities as, for example, shock waves in gas dynamics [19, 33]. The investigations showed that it is advantageous to represent the problem of a moving front by a problem

with a free boundary. This means the front is described by a moving boundary with adequate boundary conditions. The formulation of these boundary conditions is easily performed in the (q, T) coordinate system in contrast to the (x, t) system. In general, the boundary conditions may be formulated by means of the starting differential equation. In the present case, taking into account $\partial u/\partial T = 0$ at the boundary q_i, the boundary condition can be expressed by the following differential relation

$$\frac{\partial P(u)}{\partial q} + \frac{\partial (Qu)}{\partial q} = 0, \qquad q = q_i = 0.3 \tag{36}$$

from which the velocity of the moving front can be derived after approximating (36) by a difference equation.

As for Example 1, the Burgers' equation, together with conditions (32) and (33), has been solved first in the (x, t) coordinate system on a fixed grid. In Fig. 5, the solution obtained on a uniform grid with 1500 points is shown at different times. The solution develops rapidly into a stationary state which corresponds to a moving step. At the front, considerable erroneous oscillations appear which cannot be avoided simply by increasing the number of grid points. For this reason the problem has been solved alternatively by using the present adaptation procedure. In this way, a solution without oscillations has been obtained for only 16 grid points as shown in Fig. 6 where the solution of equations (22) and (11) subject to conditions (32) – (36) has been plotted. Thus, also in this second example, the dispersion of the difference scheme is strongly suppressed due to the dynamical adaptation.

In both examples considered, the solutions are characterized by one region with a very large gradient and other regions with small gradients. In the case of dynamically adaptive grids, this can lead to a strongly non–uniform grid point density up to the complete disappearance of grid points in the regions of small gradients (cf. Fig. 7). There are several possibilities to avoid this effect:

(i) If the ratio of the maximum and minimum grid point density exceeds a certain limit, the grid point with the minimum value of Ψ_i is removed and is added to the region with the maximum value of Ψ_{i+1}/Ψ_i. In the considered examples, the relation $\Psi_{i+1}/\Psi_i >$ 10 to 100 has been used as a criterion for a grid point rearrangement.

(ii) The function Q is modified by an additional term $-D\,\partial\Psi/\partial q$ which tends to equalize the grid point density [18]. The numerical parameter D has to be chosen suitably in order to slow down the grid point movement but not to suppress adaptation completely.

A series of numerical calculations revealed that the mechanism of dynamical adaptation does not depend sensitively on the special choice of the function Q. Application of the simple formula (21) for Q in the above examples demonstrated that the numerical dispersion was sufficiently suppressed. The use of formula (12), which fulfills the stationary condition (5) exactly, showed the same behaviour, only the grid point movement was slightly modified.

The calculations confirmed also the theoretical prediction that dynamical adaptation may be applied with equal success to explicit and implicit difference schemes. Only the computational efficiency differs owing to different time increments during integration. In

Fig. 8, the time increments τ for different difference schemes are compared to each other as well as to the maximum time increment τ_c which follows from the well–known stability requirement of the explicit difference scheme (Courant condition and the corresponding condition for diffusive problems). The comparison of the curves shows that the explicit scheme requires a considerably smaller time increment than the implicit schemes. Implicit schemes of order $O(\tau + h)$ and $O(\tau + h^2)$ yield practically the same results. The Crank–Nicholson scheme of order $O(\tau^2 + h^2)$ permits calculations with a time increment τ about two times larger than schemes of first order. However, the number of arithmetic operations is also two times larger in this case. Thus, in summary, the method of dynamical adaptation actually depends only weakly on the accuracy of the difference scheme.

5 Concluding remarks

In the following, essential advantages of the proposed adaptive grid method are listed:

1. An optimal movement of grid points has been achieved by an appropriate TDCT determined by the condition that in the computational space the solution behaves nearly stationary. Numerical calculations suggested that the method is relatively insensitive to the special choice of the function Q determining the TDCT (cf. eqs. (3) and (4)) provided the time derivative of the field in the computational space is sufficiently reduced by the transformation.

2. An analytical and numerical analysis of the presented solution procedure for the case of the Burgers' equation revealed that the properties of explicit and implicit finite–difference schemes are essentially improved. The dynamical adaptation leads to a decrease of the dispersion and dissipation of the difference scheme and, therefore, only a small number of grid points is needed compared to calculations on a fixed grid. As a consequence, the computational efficiency of the present method is sufficient for practical applications although the grid movement is calculated at every time step.

3. The general formulation of the dynamical adaptation procedure by differential equations permits also to apply the finite–element method for a numerical solution.

4. The idea of the present method is quite general and can serve for the generation of dynamically adaptive grids for a wide class of evolution equations including two– and three–dimensional problems.

References

[1] Numerical Grid Generation, ed. J. F. Thompson, North–Holland, Amsterdam 1982.

[2] J. F. Thompson, AIAA J. 22, 1505 (1984).

[3] M. J. Berger and P. Colella, J. Comput. Phys. 82, 64 (1989).

[4] S. Acharja and F. H. Moukalled, J. Comput. Phys. 91, 32 (1990).

[5] A. J. Wathen, J. Comput. Phys. 101, 51 (1992).

[6] R. Biswas, J. E. Flaherty and D. C. Arney, Appl. Numeric. Mathematics 11, 259 (1993).

[7] J. F. Thompson, Z. U. A. Warsi and C. W. Mastin, J. Comput. Phys. 47, 1 (1982).

[8] J. U. Brackbill and J. Saltzman, J. Comput. Phys. 46, 342 (1982).

[9] D. A. Anderson, Appl. Mathem. Comput. 24, 211 (1987).

[10] K. Matsuno and H. A. Dwyer, J. Comput. Phys. 77, 40 (1988).

[11] N. N. Yanenko, V. M. Kovenja, V. V. Lisejkin, V. M. Fourin and E. V. Vorozhtsov, Comput. Methods Appl. Mech. Eng. 17/18, 659 (1979).

[12] J. B. Bell and G. R. Shubin, J. Comput. Phys. 52, 569 (1983).

[13] M. M. Rai and D. A. Anderson, AIAA J. 20, 496 (1982).

[14] R. J. Gelinas, S. K. Doss and K. Miller, J. Comput. Phys. 40, 202 (1981).

[15] K. Nakahashi and G. S. Deiwert, AIAA J. 25, 513 (1987).

[16] J. G. Verwer, J. G. Blom and J. M. Sanz–Serna, J. Comput. Phys. 82, 454 (1989).

[17] N. A. Dar'in and V. I. Mazhukin, DAN USSR 298, 64 (1988).

[18] N. A. Dar'in and V. I. Mazhukin, Differential Equations 23, 1154 (1987).

[19] N. A. Dar'in, V. I. Mazhukin and A. A. Samarskii, DAN USSR 302, 1078 (1988).

[20] V. I. Mazhukin and L. Ju. Takoeva, J. Math. Modelling 2, 101 (1990).

[21] E. R. Benton and G. W. Platzman, Quart. Appl. Mathem. 30, 195 (1972).

[22] D. A. Anderson, J. C. Tannehill and R. H. Pletcher, Computational Fluid Mechanics and Heat Transfer, New York 1984, p. 384.

[23] P. A. Gnoffo, AIAA J. 21, 1249 (1983).

[24] K. Nakahashi and G. S. Deiwert, AIAA J. 6, 948 (1986).

[25] H. Reiger, U. Projahn and H. Beer, Int. J. Heat and Mass Transfer 25, 137 (1982).

[26] M. Lacroix and A. Garon, Numerical Heat Transfer, Part B. 19, 57 (1992).

[27] M. B. Aston and J. W. Thomas, in Numerical Grid Generation, ed. J. F. Thompson, North–Holland, Amsterdam 1982, p. 909.

[28] R. W. Yeung, Annual Review on Fluid Mechanics, 21, 395 (1982).

[29] V. F. Vasilevsky and V. I. Mazhukin, Differential Equations 25, 1178 (1989).

[30] P. V. Breslavsky and V. I. Mazhukin, Eng. Phys. J. 57, 107 (1989).

[31] R. E. Warming and B. J. Hyett, J. Comput. Phys. 14, 159 (1974).

[32] Ju. I. Shokin, First Differential Approximation, Nauka, Novosibirsk 1979.

[33] V. F. Vasilevsky and V. I. Mazhukin, Preprint Keldysh Inst. Appl. Mathem. N 14, 1989.

Captions

Figure 1: Numerical solution for Example 1 with a conventional calculation on a fixed grid with 1000 points showing oscillations at the moving front (t_i = 0, 0.1, 0.2, 0.3, ... 0.8, $\mu = 10^{-4}$).

Figure 2: Calculation as in Fig. 1 on a grid with 10 000 points (t_i = 0, 0.2, 0.3, 0.4, 0.6 and 0.8).

Figure 3: Numerical solution for Example 1 with a calculation on a dynamically adaptive grid with 25 points (t_i = 0, 0.2, 0.4, 0.6 and 0.8).

Figure 4: Parameter $\Psi = \partial x/\partial \zeta$ characterizing the distribution of grid points for the calculation in Fig. 3.

Figure 5: Numerical solution for Example 2 with a conventional calculation on a fixed grid with 1500 points showing oscillations at the moving front ($\mu = 10^{-4}$).

Figure 6: Numerical solution for Example 2 with a calculation on a dynamically adaptive grid with 15 points.

Figure 7: Parameter $\Psi = \partial x/\partial \zeta$ characterizing the distribution of grid points for the calculation in Fig. 6.

Figure 8: Comparison of time increments, τ, for different difference schemes. τ_c denotes the maximum time increment resulting from the stability requirement of the explicit scheme.

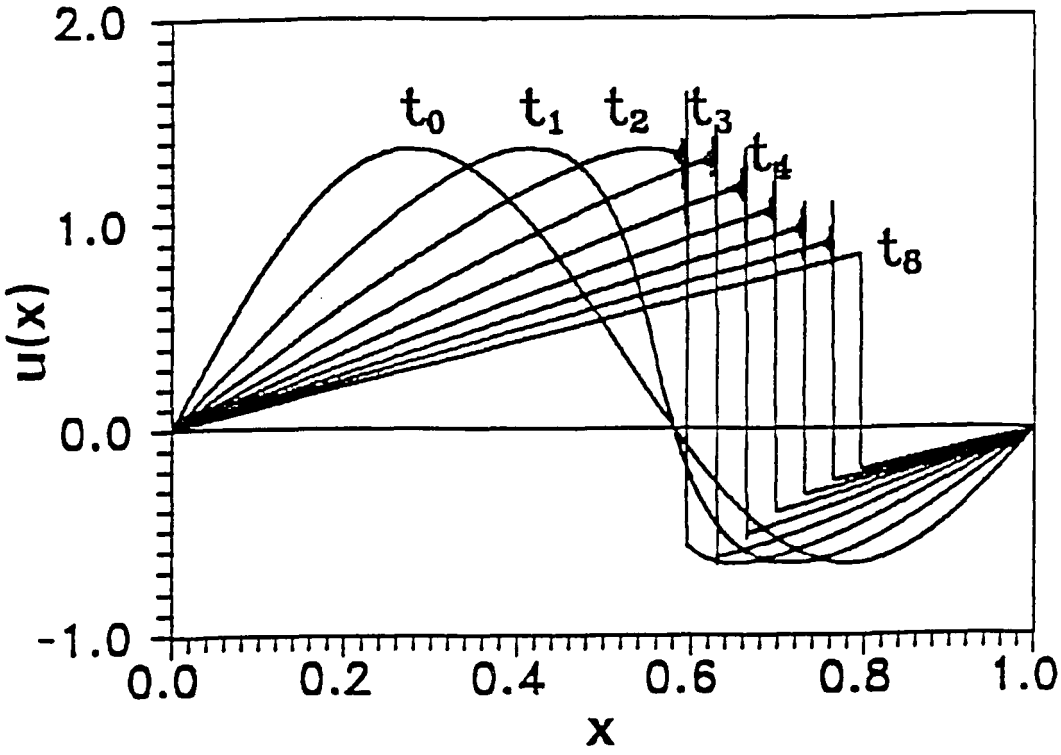
2.0
1.0
0.0
-1.0
u(x)
0.0
0.2
0.4
0.6
0.8
1.0
x
t_0
t_1
t_2
t_3
t_4
t_8

Fig. 1

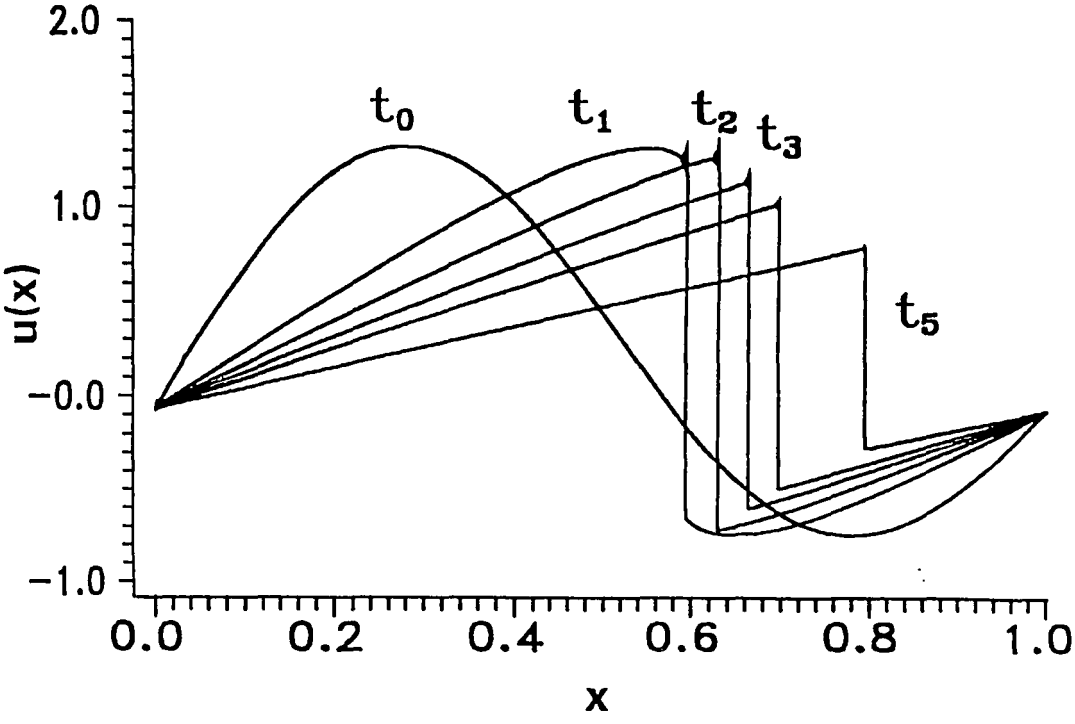
2.0
1.0
−0.0
−1.0
u(x)
0.0
0.2
0.4
0.6
0.8
1.0
x
t_0
t_1
t_2
t_3
t_5

Fig. 2

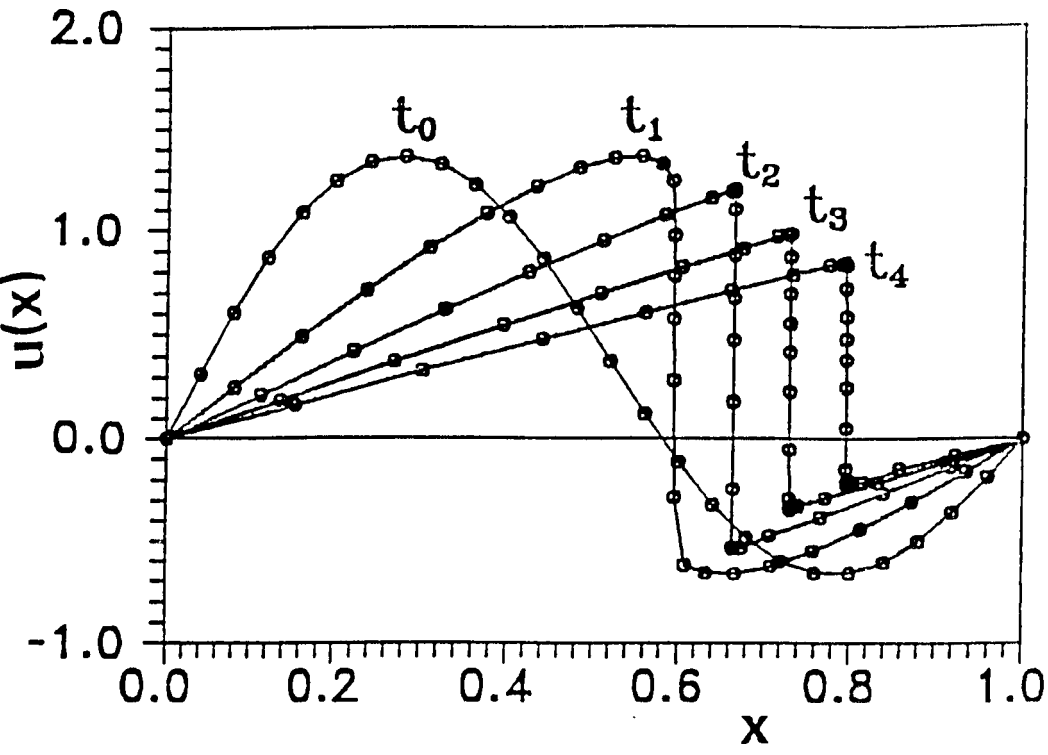
2.0
1.0
0.0
-1.0
u(x)
0.0
0.2
0.4
0.6
0.8
1.0
x
t_0
t_1
t_2
t_3
t_4

Fig.

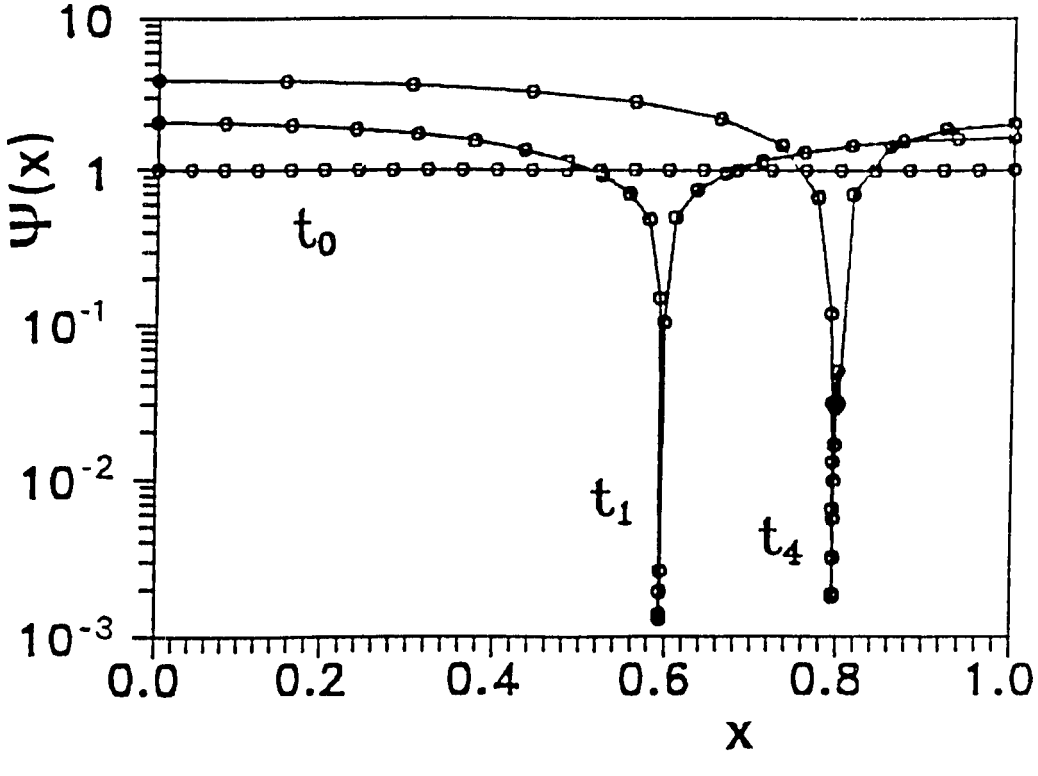
10
1
10^{-1}
10^{-2}
10^{-3}
ψ(x)
0.0
0.2
0.4
0.6
0.8
1.0
x
t_0
t_1
t_4

Fig

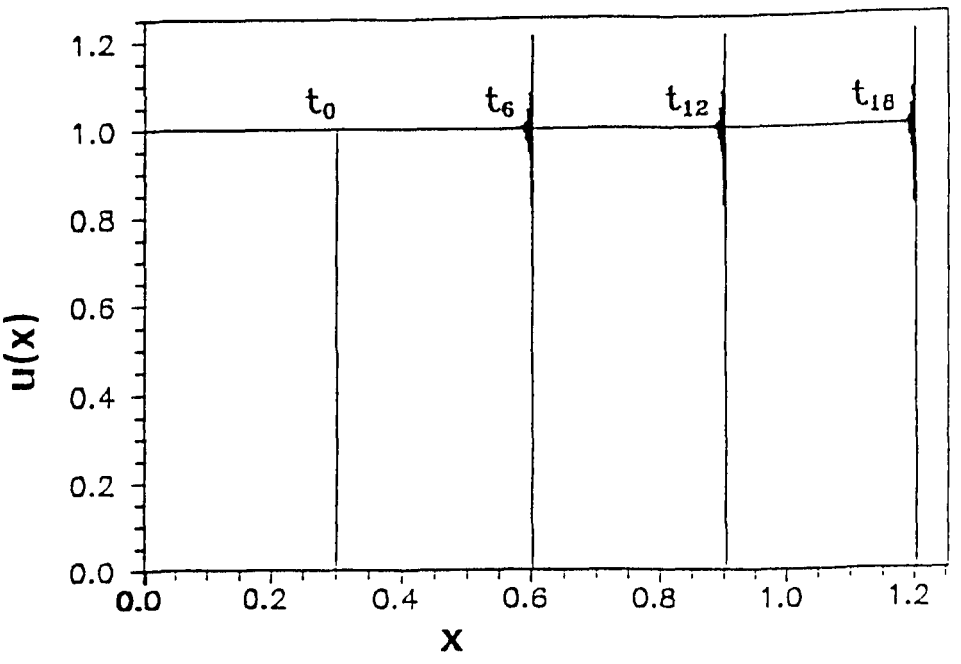
1.2
1.0
0.8
0.6
0.4
0.2
0.0
u(x)
t_0
t_6
t_{12}
t_{18}
0.0
0.2
0.4
0.6
0.8
1.0
1.2
x

Fig. 5

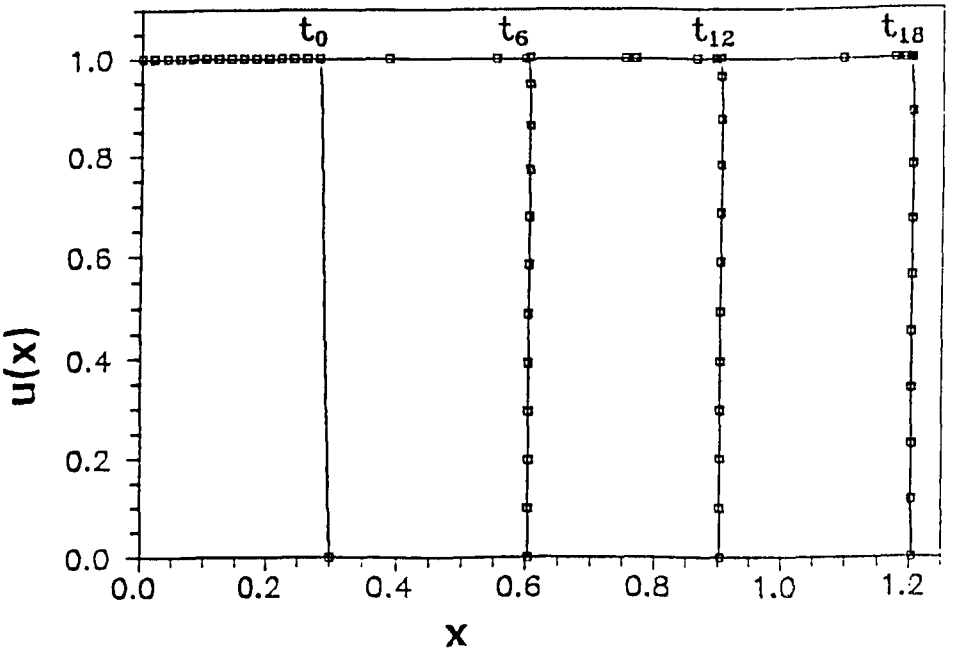
1.0
0.8
0.6
0.4
0.2
0.0
u(x)
t_0
t_6
t_{12}
t_{18}
0.0
0.2
0.4
0.6
0.8
1.0
1.2
x

Fig. 6

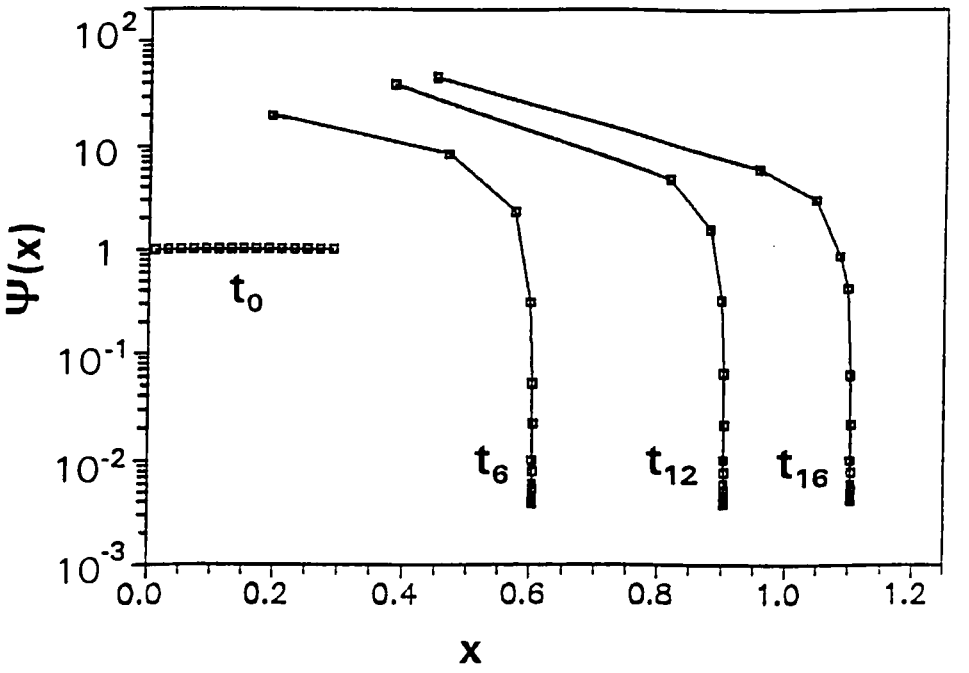
10^2
10
1
10^{-1}
10^{-2}
10^{-3}
ψ(x)
t_0
t_6
t_{12}
t_{16}
0.0
0.2
0.4
0.6
0.8
1.0
1.2
x

Fig. 7

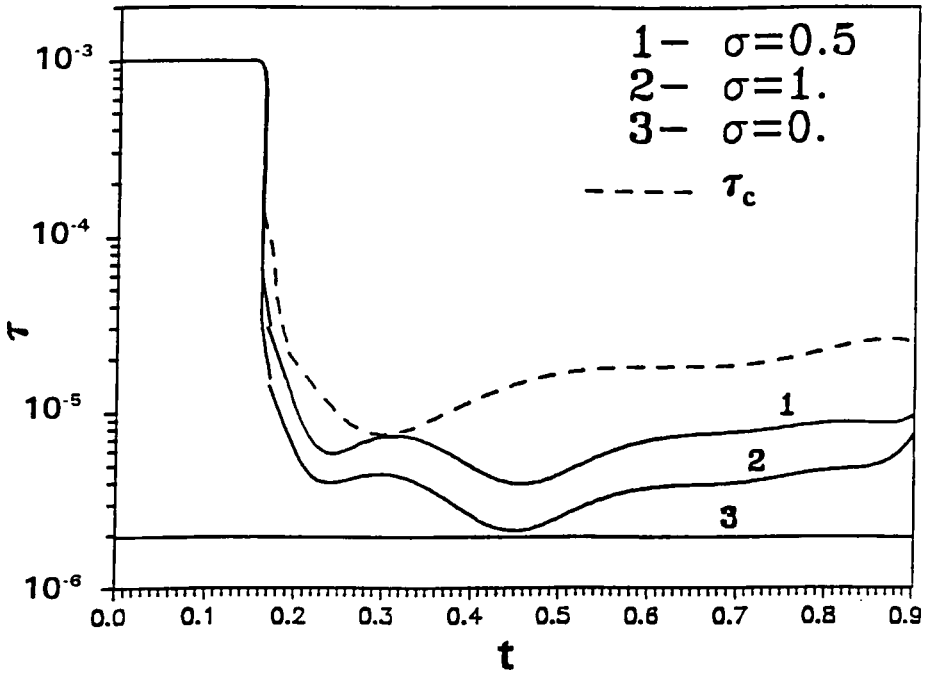
1− σ=0.5
2− σ=1.
3− σ=0.
---- τ_c
10^{-3}
10^{-4}
10^{-5}
10^{-6}
τ
1
2
3
0.0
0.1
0.2
0.3
0.4
0.5
0.6
0.7
0.8
0.9
t

Fig. 8